

Comparison in Power Consumption of Static and Dynamic WDM Networks

A. Leiva, J.M. Finochietto, B. Huiszoon, V. López, M. Tarifeño, J. Aracil, and A. Beghelli

Abstract— Greening of the Internet has become one of the main challenges for the research community. Optical networks can provide an energy efficient solution, but it has become crucial to assess its power efficiency. In this context, dynamic operation of WDM networks is expected to provide significant power savings when compared to static operation; however, its benefits need to be evaluated to determine its actual impact and to analyze future trends. In this paper, a general framework for evaluating energy consumption in WDM networks is introduced. The proposed framework enables the analysis of different node architectures, link capacities and network topologies. In particular, the case of three different node architectures is discussed and compared. Results show that dynamic operation can significantly reduce power consumption when either the traffic load is below 0.4 or when short reach transponders consume significantly lower power than long reach ones. In the latter case, dynamic operation shows significant benefits compared to the static case for traffic loads higher than 0.4. It is also shown that the transponders of the input/output stage of the nodes determine the benefit –in terms of power consumption– of an eventual migration from static to dynamic architecture rather than the transponders of the interface between the WDM and higher layers.

Index Terms— Optical networks, energy efficiency, power consumption.

I. INTRODUCTION

OPTICAL WDM networks is the only technology that can absorb the ever-growing traffic demand. Currently, most lightpath allocation in the WDM layer is carried out statically [1]. However, due to the ability to adapt to traffic and topology changes, a dynamic WDM layer would yield

Manuscript submitted July 06, 2010.

This work was supported by the UAM-Banco Santander CEAL grant, the “Juan de la Cierva” postdoctoral research grant from The Spanish Ministry Ministerio de Ciencia e Innovación (MICINN), DGIP-UTFSM Scientific Initiation Scholarship, Conicyt and DGIP-UTFSM Scholarships for PhD studies, USM Project 23.09.70 and Centro Científico Tecnológico Valparaíso Project #FB/28AB/10.

A. Leiva, A. Beghelli, and M. Tarifeño are with the Telematics Group, Electronic Engineering Department, Universidad Técnica Federico Santa María, Valparaíso, Chile (E-mail: alejandra.beghelli@usm.cl). A. Beghelli is also Honorary Research Associate of the Electronic & Electrical Eng. Dept, UCL, UK and A. Leiva is with the Telecommunications Group, Electrical Engineering School, Pontificia Universidad Católica de Valparaíso, Chile (E-mail: ariel.leiva@ucv.cl).

J.M. Finochietto is with the Digital Communications Research Lab, Universidad Nacional de Córdoba-CONICET, Córdoba, Argentina (E-mail: jfinochietto@efn.unicor.edu)

B. Huiszoon, V. López, and J. Aracil are with the High Performance Computing and Networking Research Group, Escuela Politécnica Superior, Universidad Autónoma de Madrid, 28049, Madrid, Spain (E-mail: bhuiszoon@ieee.org).

significant cost savings in terms of capital and operational expenditure (CapEx and OpEx) terms with respect to the static approach. Therefore, during recent years the research community has made a huge effort to provide dynamic operation to optical networks. A main step in this direction has been the improvement in the control plane (GMPLS, ASON), which allows network operators to dynamically change the configuration of their systems [2, 3].

The effect of dynamic and static operation in the CapEx of WDM networks (in terms of wavelength requirements) was first studied in [4-6]. From these studies it was found that dynamic operation requires a lower number of wavelengths than static operation in a wide range of traffic loads only if wavelength conversion is provided. It is therefore that the dynamic nodes studied here contain wavelength converters.

One of the current challenges of the telecommunications industry and research community is to provide energy-efficient solutions [7]. This will certainly have an impact not only in its OpEx but as well in the demand that telecommunication networks impose on the energy generation system (some studies have raised the power consumption of telecommunication infrastructure up to 10% of the world consumption [8]). Optical networks are again positioned as a key technology to solve such power consumption problem.

Authors in [9-11] show that optical networks power consumption is lower than that of traditional routers. Given that a migration from static to dynamic WDM operation is widely expected, studying the potential benefits of dynamic operation in terms of power consumption with respect to the static approach becomes a key task.

The CapEx of IP over WDM networks is analyzed for static and dynamic WDM operation in [11], however, the power consumption analysis is done only for a static WDM layer. In [12], the case of power saving network architectures for unidirectional WDM rings is considered. The study evaluates different node architectures following a simpler approach to the one proposed in this paper. An AWG-based switching architecture is combined with wavelength tuneability in [13]. In this work, a similar node architecture is considered; however, long-haul transmission with signal regeneration at the node is permitted here.

Traffic engineering techniques are employed in a recent work to switch off links with low loads, and thereby achieving energy savings [14]. Traffic is rerouted on links that have spare capacity. All-optical 3R regeneration is also considered to avoid using the electrical domain for this purpose. However, the advantage of 3R over standard optical-electrical-optical (OEO) regeneration is not justified in terms of power

consumption as values in the kilowatt range are reported. As a result, in this work standard OEO is considered.

As most previous works focus on the power consumption of higher layers (mainly, layer 3, in charge of routing), the contribution of this work is the comparison of the power consumption of the physical WDM layer under static and dynamic operation. To do so, three node architectures are characterized and compared in terms of power consumption: (1) a classical static WDM node, (2) a low-consumption static WDM node and (3) a dynamic WDM node. We expect dynamic WDM nodes to consume significantly lower power than either of the two static approaches because of lower wavelength and transmitter/receiver requirements. The reduction of the number of wavelengths decreases the size of commutation devices (port-count) and the number of wavelengths converters in the network nodes.

In this paper an extensive analysis of power consumption of static and dynamic WDM networks has been made, providing an in-depth comparison of several node architectures and considering the usage of lightpaths in the network. We expect that the results presented here may help network operators make a decision to potentially migrate from static to dynamic operation of WDM networks.

The remainder of this paper is organized as follows. Section II describes the network and traffic models for static and dynamic WDM operation. The node and link equipment used for each WDM networks cases are presented in Section III. Section IV describes the power consumption model for each architecture. Section V presents the numerical results for four topologies operating as static and dynamic WDM networks and, finally, Section VI concludes the paper.

II. NETWORK AND TRAFFIC MODELS

A. Network models

a) Network architectures

The static WDM network considered in this paper assumes that a lightpath between each pair of electronic routers must be established in a quasi-permanent basis, as in [15]. Thus, network resource configuration does not change during network operation.

The dynamic WDM network considered in this paper assumes end-to-end reservation of lightpaths on demand (e.g. end-to-end optical burst switching [16], optical flow switching [17]), as it has been shown to achieve a much lower blocking probability than hop-by-hop reservation mechanisms [18] as well as a lower power consumption than packet switching approaches [9]. In such a network, once a condition (established a priori) for data transmission is met, a control packet is sent through the network to reserve and to configure transmission resources (transmitters, receivers and optical crossconnects) in an end-to-end basis.

b) Network model

The WDM network is represented by the graph $G=(\mathcal{N}, \mathcal{L})$, where \mathcal{N} is the set of nodes (each node corresponds to an electronic router locally attached to an optical node) and \mathcal{L} is

the set of unidirectional links. The cardinality of sets \mathcal{N} and \mathcal{L} is denoted by N and L , respectively. We assume a space-division full-duplex scenario; thus, between each pair of adjacent nodes there is one cable, made of two unidirectional links (fibers), one in each direction. The capacity required by link $l \in \mathcal{L}$ (in number of wavelengths) is represented by W_l . In the static WDM network, W_l represents the number of lightpaths using the link l . In the dynamic WDM network, W_l is determined by a dimensioning process that takes into account the traffic load and the maximum acceptable blocking probability per connection [4]. The number of transmitters and receivers required in node $n \in \mathcal{N}$ is denoted by TR_n . Assuming that every node requires a lightpath to all remaining nodes, in the static case $TR_n = 2 \cdot (N-1)$, as each node is equipped with $N-1$ transmitters and $N-1$ receivers. In the dynamic case, the number of transmitters and receivers per node is determined by applying a dimensioning process that takes into account the traffic load and the blocking probability per connection. This computation is explained in Section V.

B. Traffic model

Let C be the set of connections in the network. Each connection $c \in C$ corresponds to a specific source-destination pair. Each connection is assumed to generate traffic according to an ON-OFF process. We assume that during the ON period, the source node of connection c transmits at the wavelength bit rate of b . During the OFF period, the source refrains from transmitting data. The mean duration of the ON(OFF) period is denoted by t_{ON} (t_{OFF}). The traffic load offered by each individual connection, ρ , is then given by:

$$\rho = \frac{t_{ON}}{t_{ON} + t_{OFF}} \quad (1)$$

In the static operation case (see, for example [15], [19], [20]), a lightpath is permanently allocated to each connection with $\rho > 0$. Thus, the number of lightpaths to allocate between source node i and destination node j , $T[i, j]$, is given by the following expression:

$$T[i, j] = \lceil \rho \rceil \quad (2)$$

Where $\lceil x \rceil$ represents the lowest integer greater than or equal to x .

In this paper we assume that every node pair has a traffic load higher than zero. Thus, in the static case, a lightpath must be established between each pair of nodes.

III. NODE AND LINK EQUIPMENT

A. Optical node equipment

a) Static WDM network

Two node architectures, shown in Figure 1 and 2, are considered for the static WDM network. Both node architectures can deal with a different number of wavelengths per fiber and are made of four sections: the interface between the electronic router and the optical node (made of fixed transmitters/receivers in charge of adding/dropping traffic),

the input stage (in charge of de-multiplexing and directing the passing-through traffic to the commutation device), the commutation stage and the output stage.

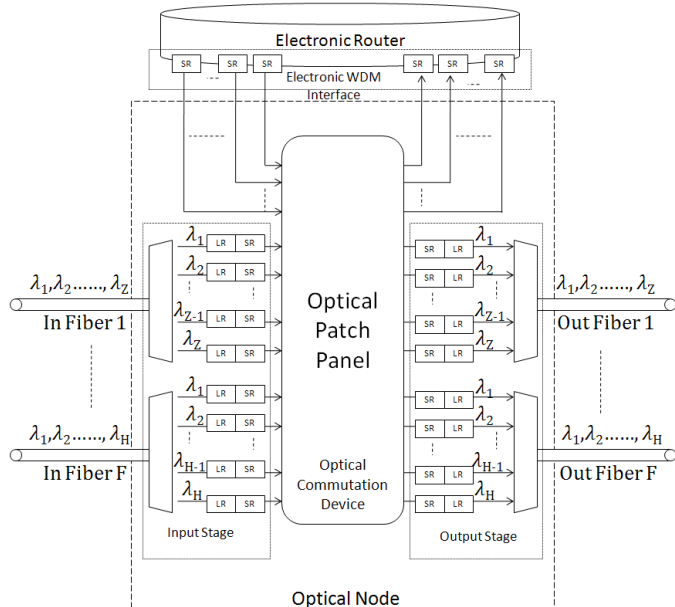


Figure 1: Static classic optical node (SCON) architecture.

The first design is referred to as Static Classic Optical Node (SCON). In this architecture, the electronic router is connected to a passive optical patch panel by fixed short-reach (SR) transmitters/receivers (N-1 transmitters and N-1 receivers). The transmitters are in charge of transforming the electronic signal coming from the electronic layer into the optical domain of the WDM layer. Conversely, the receivers transform the optical signal from the WDM layer into the electronic format required by the electronic layer. The optical data passing through the optical node (without being electronically processed by the electronic layer) is received by the input stage, where the incoming optical signal is first demultiplexed and then regenerated by long-reach (LR) receivers/short-reach (SR) transmitters (transponders of input stage). Next, the regenerated signal is transmitted through the commutation device. After commutation, the optical signal is once again regenerated by a pair of short-reach receiver/long-reach transmitter (transponders of output stage) and multiplexed into the output fiber. The transponders of the input and output stages could also be used as wavelength converters.

The following text focuses on the electronic WDM interface shown in Figure 1. Given that the optical signals generated by the node itself do not need to go through additional regeneration stages, some of the output ports of the commutation device (those used to transmit the signals generated at the node) do not need transponders at the output stage. Additionally, incoming signals have already been regenerated at the output stage of the previous node and amplified by the amplification stages in the link. Therefore, there is no need for regeneration at the input stage.

A second node design is shown in Figure 2 that aims for

improvement in terms of energy consumption. It is referred to as the Static Low-consumption Optical Node (SLON). In this architecture the input stage does not have any regenerator or transponder. This task is performed exclusively during the output stage. In the interface stage, the electronic router is connected to a passive optical patch panel by long-reach (LR) transmitters/receivers (N-1 transmitters and N-1 receivers). By changing the short-reach transmitters of the interface stage of the SCON architecture for long-reach transmitters, some regenerators (transponders) of the output stage can also be eliminated (as shown in the output stage of Figure 2) since the signals originating in the node do not need go through a regeneration process when they leave the optical patch panel.

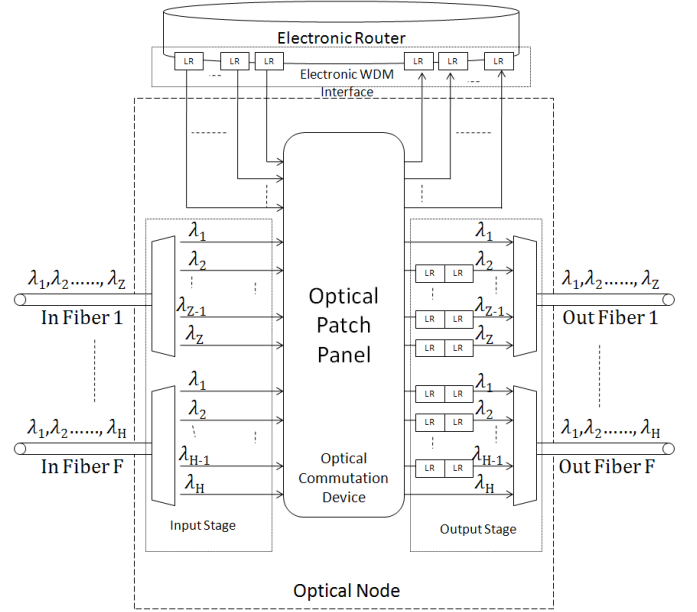


Figure 2: Static low-consumption optical node (SLON) architecture.

b) Dynamic WDM network

Figure 3 shows the dynamic optical node (DON) architecture for the WDM layer. The main differences with respect to the case of a static WDM layer are:

- The interface between the electronic layer and the optical node, where the transmission is carried out by short-reach tuneable transmitters.
- The input stage is now made of tuneable LR-SR transponders, with wavelength conversion capability.
- The optical commutation device is based on passive arrayed waveguide gratings (AWGs) as in [21], whose input-output relationship is fixed for each wavelength at a port.
- The output stage is made of fixed SR-LR transponders with wavelength conversion capability. A fixed wavelength converter has a fixed output wavelength for any input wavelength.

In the dynamic node, passing traffic is de-multiplexed, converted to a different wavelength, if necessary, by means of a LR-SR tuneable transponder. It is then directed to the destination output fiber along with the added traffic or

dropped by means of a passive AWG. At the output of the AWG, the signal is converted by means of a fixed wavelength converter, such as the SR-LR fixed transponder. Transponders are used as optoelectronic wavelength converters.

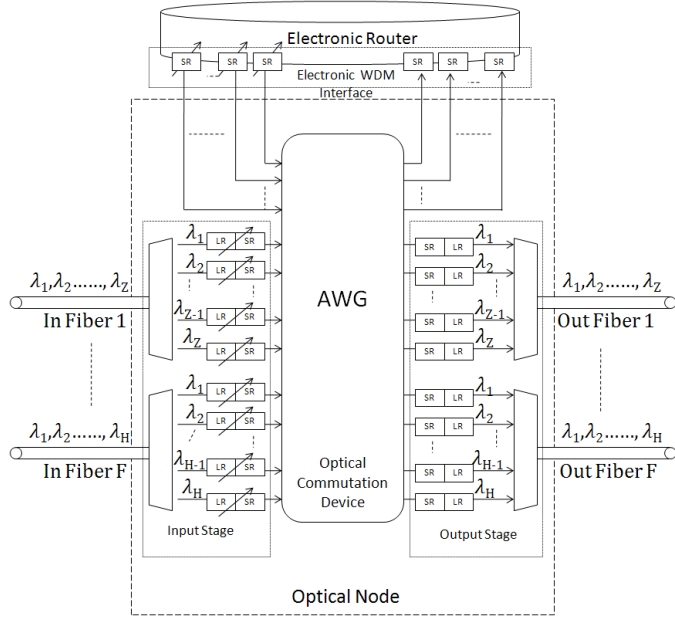


Figure 3: Dynamic optical node (DON) architecture.

The central AWG in Figure 3 may be replaced a micro-electro-mechanical systems (MEMS)-based commutation device if reconfigurability is required inside the node. Recall that an AWG routes light signals from input to output based on the wavelength and the input port, therefore providing fixed paths. A MEMS-based commutation device allows any wavelength to switch to any output port. However, the established path should remain permanently active for the duration of a lightpath. The reader should note that a MEMS-based DON also requires tuneable SR transponders in order to enable dynamic lightpath allocation at the WDM layer. Additionally, short-range transponders can be required to compensate for the losses of the commutation (switching) device whether it is an AWG or a MEMS. In [22], a comprehensive overview of MEMS-based optical crossconnects is provided as well as a list of some power consumption figures. For example, an 80x80 MEMS-based switch has been demonstrated that only consumes 8.5 W, so replacing the AWG by a MEMS-based commutation device is not expected to significantly impact the power consumption of a DON. In conclusion, the schematic design in Figure 3 may also represent a MEMS-based DON, however it may add additional signaling overhead considering the reconfigurability of the MEMS.

B. Link equipment

Network links spanning hundreds of kilometers require signal regeneration because of accumulated linear and non-linear effects caused by the optical fiber. Typically, a link is constructed by several spans of fiber, and optical amplifiers are used to compensate for the transmission losses of each

span. The most widespread configuration uses Erbium-doped fiber amplifiers (EDFAs) to all-optically amplify the whole incoming wavelength-comb. As a result, the total power consumption of each transmission link between nodes is directly related to the number of required EDFAs. If the number of required EDFAs and/or their power consumption do not significantly change between static and dynamic operation scenarios, then the power consumption of links becomes irrelevant in this work (since we focus on a comparison between the power consumption of the static and the dynamic case rather than an exact evaluation of it). It is assumed that all EDFAs operate in the well-known automatic gain control (AGC) mode with one or more control loops to resolve gain transients as a consequence of channel dynamics. Ref. [23] shows a typical configuration of a two-stage EDFA including a lossy gain flattening filter and a variable optical attenuator placed in the middle of the two Erbium-doped fiber sections. Each of the sections are pumped at a different wavelength, namely at 980 nm and 1480 nm. That particular EDFA configuration is used in the remaining of this section.

In this paper, the simplified link architecture of Figure 4 is considered. This is made of a multi-channel transmitter (Node A) followed by a booster EDFA, a transmission link consisting of one or more spans with in-line EDFAs, and finally the receiver (Node B). The total number of EDFA's N_{EDFA} is given by

$$N_{\text{EDFA}} = \lceil L_{AB}/K \rceil + 1 = M + 1 \quad (3)$$

where L_{AB} is the total link length between node A and B, K the span length, and M the number of spans. The reader should note that the in-line EDFA of the last span acts as the pre-amplifier of the receiver.

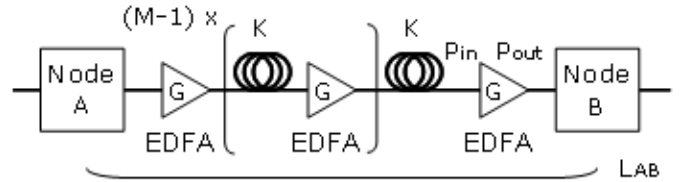


Figure 4: Schematic of a typical fiber-optic transmission link.

The value of M also determines the span length because it is closely related to the link budget. If $M=1$, the high output power of the booster EDFA and the high sensitivity of the pre-amplifier allow a single span of several hundred km [24]. If $M>1$, a span typically has a lower fixed length which is commonly taken equal to 80 km in metro/core networks with the last span being of any length. For the rest, a SSMF fiber with an attenuation of 0.25 dB/km is assumed.

In the following section, the EDFA's response to channel add/drop is analyzed in terms of its power consumption. For this purpose, several parameters are defined; namely: the number of wavelength channels N_{ch} , the attenuation coefficient α in dB/km, the EDFA gain G in dB, the EDFA total output power P_{out} in dBm, the EDFA output power per channel $P_{\text{out},\text{ch}}$ in dBm, and the EDFA input power per channel

$P_{in,ch}$ in dBm.

Each optical channel is degraded by the span losses $\alpha \cdot K$, and therefore $P_{in,ch}$ is given by $P_{in,ch} = P_{out,ch} - \alpha \cdot K$ with the $P_{out,ch}$ taken from the previous EDFA. The value of $P_{out,ch}$ at the output of each EDFA is the same across L_{AB} so each EDFA fully compensates for the span losses ($= \alpha \cdot K$) by means of its gain G . In that case, the total input power at each EDFA in the link equals to $P_{in} = P_{out,ch} + 10 \cdot \log_{10}(N_{ch}) - \alpha \cdot K$, and $P_{out} = G \cdot P_{in}$. So link design is governed by the limiting values for G , $P_{out,ch}$ and P_{out} for a given type of amplifier. Basically, a lower N_{ch} leads to a lower required P_{out} if $P_{out,ch}$ and G are kept constant at the EDFA. This is achieved through the AGC mechanism which adjusts the driving conditions, that is, AGC adjusts the bias current of the pump laser(s) when the input power suddenly changes [25]. Therefore, in the case of a lower amount of input channels, the EDFA should have lower electrical power consumption as well.

The output powers of the two pump lasers at 980 nm and 1480 nm can be estimated through their power conversion efficiency (PCE) as follows:

$$\eta_\lambda = (P_{out,\lambda} - P_{in,\lambda}) / P_{p,\lambda} \quad (4)$$

with $P_{out,\lambda}$ and $P_{in,\lambda}$ as the output and input power of the Erbium-doped stage in mW, and $P_{p,\lambda}$ as the output power of the pump laser in mW [25].

The following calculations have been done purely for modelling purposes and without the intention to be exact. The launch powers of the pump lasers can be estimated by evaluating the power budget from the input to the output using the EDFA shown in [23] and by applying Eq. (4). If no measured characteristics are available, datasheets of commercially available cooled pump lasers can be used to find the corresponding electrical power consumption of the laser and the thermo-electric cooler unit. For example, references [26] and [27] have data on both types of cooled pump lasers used in the EDFA model of [23]. Using that data, the results are plotted in Figure 5 for when the static network is designed to operate with a maximum of 20 or 80 wavelength channels ($N_{ch,max} = \{20, 80\}$).

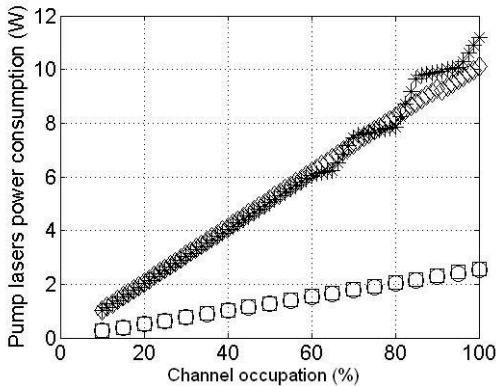


Figure 5: Indicative electric power consumption of EDFA pump lasers for a varying amounts of input channels in the case of $N_{ch,max}=20$ (circle: [26], square: [27]) and $N_{ch,max}=80$ (star: [26], diamond: [27]).

The channel occupation at the x-axis of Figure 5 is the ratio between the number of active channels divided by $N_{ch,max}$. The pump lasers of both [26] and [27] appear to have similar power consumption results in both cases. Furthermore, it is shown that the electrical power consumption of an EDFA may be approximated by the a linear expression as follows

$$P_{EDFA} = A + B \cdot N_{ch} \quad (5)$$

with P_{EDFA} in mW, A the average power consumption of the host, and $B = b_1 + b_2$ as the average power consumption per channel where b_1 and b_2 represent the contributions of the optics and the electronics. The host refers to the large amount of electronics that provision, for example, AGC management, communication and control interfaces, laser temperature control, and powering. The reader should note that the parameters A and b_2 are equal to zero in Figure 5. Regarding factor b_1 , the linearity represents the EDFA's flat gain, for example as shown in [28], which may be intuitively understood as follows: To achieve a flat gain, the average inversion (or: PCE) is kept at a constant level for any pump and input power. Furthermore, the pump lasers are typically operated in the linear regime. Regarding the factor b_2 , electronic signal processing is typically done per channel. A more elaborate modeling may be required when taking b_2 into account.

This analysis will be used in section V to evaluate whether a migration from static to dynamic operation may have an impact on the power consumption due to the EDFA in the network links. The authors note that the evaluation done above has been performed for the specific EDFA design shown in [23]; however, [25] shows many possible EDFA designs, so a more generalized model should give more conclusive results.

IV. NETWORK POWER CONSUMPTION

Let:

- W_n^{in} and W_n^{out} be the sum of the number of wavelengths of all the links that finish and start at node n , respectively. In the dynamic case they are denoted by $W_n^{in}(\rho)$ and $W_n^{out}(\rho)$, as they are dimensioned as a function of the traffic load ρ .
- W_{net} be the total wavelength-link count of the network (W_{net}^{SCON} or W_{net}^{SLOW} for the static case and W_{net}^{DON} for the dynamic case). In the dynamic case, this is denoted by $W_{net}^{DON}(\rho)$, as it is a function of the traffic load ρ . W_{net} is given by $W_{net} = \sum_{\forall l} W_l = \sum_{\forall n} [W_n^{in} + W_n^{out}]$.
- TR_n be the sum of transmitters and receivers in the electronic-WDM interface of node n . In the dynamic case, it is denoted by $TR_n(\rho)$, as the transmitters and receivers are dimensioned as a function of the traffic load ρ .
- $P_{interface}$, P_{input} , $P_{commutation}$, and P_{output} be the power consumption of the electronic-WDM interface, input, commutation and output stages, respectively.

- P_S be the power consumption of the SR transmitters or receivers (or short reach part of transponders of input or output stage).
- P_L be the power consumption of the LR transmitters or receivers (or long reach part of transponders of input or output stage).
- β be the ratio between P_L and P_S . That is, $\beta = P_L/P_S$.
- P_{SS} , P_{LL} , P_{SL} , P_{LS} be the power consumption of the SR-SR, LR-LR, SR-LR and LR-SR transponders, respectively. It is assumed that $P_{SS} = 2 \cdot P_S$, $P_{LL} = 2 \cdot P_L$, $P_{SL} = P_{LS} = P_S + P_L$. Furthermore, tuneable transponders consume as much as non-tuneable devices. The reader should note that separate SR and LR transponders in transmitters or receivers parts are used and not integrated versions, so the power consumption of each device can be summed.

In our analysis, β is a key parameter since it models the power consumption ratio of long haul optical transmissions against short reach ones when considering transponders. In today's 10-Gbps networks, the value of β is close to 1 since almost the same technology is used for both connections despite the fact that they typically operate on different wavelength windows [29]. However, it is expected that in higher speed networks (i.e., 40 or 100-Gbps) long-haul transponders could require the integration of much more electronic processing to compensate for fiber distortion effects. In particular, more complex modulation schemes as well as more sophisticated electronic dispersion compensation (EDC) techniques could be employed. Besides, the use of more complex forward error correction (FEC) codes could become necessary to offer good performance. As a result, we assume that long haul transponders could consume up to one order of magnitude more than short reach ones, which implies a value of β around 10.

The power consumption of node n , P_n , is given by:

$$P_n = P_{\text{interface}} + P_{\text{input}} + P_{\text{commutation}} + P_{\text{output}} \quad (6)$$

$P_{\text{interface}}$ corresponds to the sum of the power consumption of electronic-WDM interface transmitters and receivers; P_{input} corresponds to the sum of the power consumption of all the transponders at the input stage (if any). The power consumption of the demultiplexers is equal to zero, since they are passive elements. Since the commutation devices of the three node architectures studied in this paper are passive elements, $P_{\text{commutation}}$ is also equal to zero. Finally, P_{output} is given by the sum of the power consumption of the output stage transponders.

The power consumption of link l , P_l , is given by:

$$P_l = N_{OA,l} \cdot P_{OA} \quad (7)$$

where $N_{OA,l}$ and P_{OA} are the number of optical amplifiers in link l and the power consumed by an optical amplifier, respectively.

Therefore, total power consumption of a network is given by the sum of the power consumption of all network nodes and links.

As shown in section III.B, P_l depends on the channel reduction experienced when migrating from a static to a dynamic networking scenario.

In the following, expressions for the total power consumption (P_{nodes}) for the static and dynamic case are derived for each of the three nodes. To do so, in the static case it is assumed that all components are in an active state, irrespective of their level of utilization. In the dynamic case however, there is a traffic load-dependent channel activation mechanism that makes some components becoming inactive (stand-by mode) when not used.

SCON architecture: Let $P_{\text{nodes}}^{\text{SCON}}$ be the total power consumption of nodes of a static WDM network, equipped with nodes as that of Figure 1. Then, $P_{\text{nodes}}^{\text{SCON}}$ is given by:

$$P_{\text{nodes}}^{\text{SCON}} = \sum_{\forall n} [TR_n \cdot P_S + W_n^{\text{in}} \cdot P_{LS} + W_n^{\text{out}} \cdot P_{SL}] \quad (8)$$

Equation (8) can be simplified to:

$$P_{\text{nodes}}^{\text{SCON}} = 2 \cdot P_L \cdot \left[\frac{N \cdot (N-1)}{\beta} + W_{\text{net}}^{\text{SCON}} \cdot \left(\frac{\beta+1}{\beta} \right) \right] \quad (9)$$

SLON architecture: Let $P_{\text{nodes}}^{\text{SLON}}$ be the total power consumption of nodes of a static WDM network equipped with the SLON architecture, given by:

$$P_{\text{nodes}}^{\text{SLON}} = \sum_{\forall n} [TR_n \cdot P_L + (W_n^{\text{out}} - N + 1) \cdot P_{LL}] \quad (10)$$

Assuming that $W_n^{\text{out}} = W_n^{\text{in}}$ then Equation (10) can be simplified to:

$$P_{\text{nodes}}^{\text{SLON}} = 2 \cdot W_{\text{net}}^{\text{SCON}} \cdot P_L \quad (11)$$

DON architecture: Let $P_{\text{nodes}}^{\text{DON}}$ be the total power consumption of nodes of a dynamic WDM network equipped with the DON architecture. In this case, the values of W_l , W_{in}^n , W_{out}^n , TR_n are a function of the traffic load (and thus, they are denoted by $W(\rho)$, $W_{in}^n(\rho)$, $W_{out}^n(\rho)$, $TR_n(\rho)$). Assuming ON-OFF traffic sources, the power consumption of transmitters, receivers and wavelengths converters (transponders) depends on the duty cycle of the traffic source. During the ON period, the power consumption of each transmitter/receiver is equal to P_S while the power consumption of per wavelength converter (transponder) is equal to P_{LS} (or P_{SL}). During the OFF period, the power consumption of transmitters, receivers and wavelengths converters does not drop to zero, but rather is equal to a fraction of the power consumed during the ON period. Assuming that the power consumed during the OFF period is a fraction ε of the power consumed during the ON period, $P_{\text{nodes}}^{\text{DON}}$ is given by:

$$P_{\text{nodes}}^{\text{DON}} = \sum_{\forall n} [TR_n(\rho) \cdot P_S + W_n^{\text{in}}(\rho) \cdot P_{LS} + W_n^{\text{out}}(\rho) \cdot P_{SL}] \cdot [\rho + \varepsilon(1 - \rho)] \quad (12)$$

which can be reduced to:

$$P_{\text{nodes}}^{\text{DON}} = P_L \left[\frac{N \cdot TR_n(\rho)}{\beta} + 2 \cdot W_{\text{net}}^{\text{DON}}(\rho) \cdot \left(\frac{\beta+1}{\beta} \right) \right] \cdot [\rho + \varepsilon(1 - \rho)] \quad (13)$$

In terms of power consumption, a migration from static to dynamic operation in the WDM layer is justified only if the power consumption of the dynamic case is lower than that of the static case. That is, if:

$$\Delta_{links} + \Delta_{interface} + \Delta_{input,output} > 0 \quad (14)$$

where Δ_{links} is the difference between the power consumption of network links (i.e. $\sum_{\forall l} P_l$) for SCON or SLON and DON. $\Delta_{interface}$ and $\Delta_{input,output}$ are the difference between the values of $P_{interface}$ and $(P_{input} + P_{output})$ for the same cases. The values of such differences are calculated in the following section.

V. NUMERICAL RESULTS

The power consumption of the topologies NSFNet [4] ($N=14$ and $L=42$), EON [4] ($N=20$ and $L=78$), UKNet ($N=21$ and $L=78$) and ARPANet ($N=20$ and $L=62$), shown in Figure 6, configured as static and dynamic networks, was evaluated. In the static case, the value of TR_n was equal to $2 \cdot (N-1)$. The value of W_{net}^{SCON} is equal to that of W_{net}^{SLON} (calculated as $\sum_{\forall l} W_l$) and equal to 390, 898, 1052 and 1066 for the NSFNet, EON, UKNet and ARPANet topology, respectively. These values were obtained after applying the near-to-optimal heuristic proposed in [15] for static WDM networks dimensioning.

In the dynamic case the values of $W_l(\rho)$ and $TR_n(\rho)$ were determined so the maximum blocking probability of each connection was equal to 10^{-3} . Note that by allowing some blocking in the dynamic case and requiring zero blocking in the static case, the capacity comparison could be thought to be unfair to the static case. Conversely, if we require zero blocking for both networks, the comparison would be unfair to the dynamic case since the capacity requirements in the static case can be optimized. As a result, a dynamic network would require a significantly higher capacity than static, as shown in [30, 31]. In this paper we have chosen the first situation (allowing some blocking for the dynamic case), since the random nature of dynamic systems causes them to be designed to tolerate some blocking or data loss, as established by the ITU [32, 33].

To achieve the required value of blocking in the dynamic case, the following dimensioning heuristic was used:

- First, the same simulation-based procedure applied in [4] to determine the number of wavelengths was applied utilizing SP (Shortest Path) routing. This algorithm achieves the lowest value of wavelength requirement in wavelength-convergent networks.
- Next, once the number of wavelengths was determined, the number of transmitters and receivers per node was decreased as much as the blocking probability allowed.

Table 1 shows the dynamic network dimensioning results ($W_{net}^{DON}(\rho) = \sum_{\forall l} W_l(\rho)$ and $TR_{net}^{DON}(\rho) = N \cdot TR_n(\rho)$) for the topologies studied.

Table 2 shows the amount of channels (or: transponders) in the least and most loaded links in cases of static and dynamic wavelength handling in the NSFNet, EON, UKNet and ARPANet topologies. It is clear that the resources used are close to their maximum levels at loads of 0.4 or above.

Table 1: Wavelength, transmitters and receivers requirements for the NSFNet, EON, UKNet and ARPANet topologies under dynamic operation as a function of the traffic load.

		Traffic load								
		0.1	0.2	0.3	0.4	0.5	0.6	0.7	0.8	0.9
NSFNet	$W_{net}^{DON}(\rho)$	269	331	367	386	390	390	390	390	390
	$TR_{net}^{DON}(\rho)$	196	252	308	336	364	364	364	364	364
EON	$W_{net}^{DON}(\rho)$	490	625	725	800	850	890	898	898	898
	$TR_{net}^{DON}(\rho)$	360	480	600	640	680	760	760	760	760
UKNet	$W_{net}^{DON}(\rho)$	560	768	884	968	1021	1052	1052	1052	1052
	$TR_{net}^{DON}(\rho)$	358	502	596	698	774	830	840	840	840
ARPANet	$W_{net}^{DON}(\rho)$	544	714	832	927	1002	1034	1066	1066	1066
	$TR_{net}^{DON}(\rho)$	342	442	572	654	704	760	760	760	760

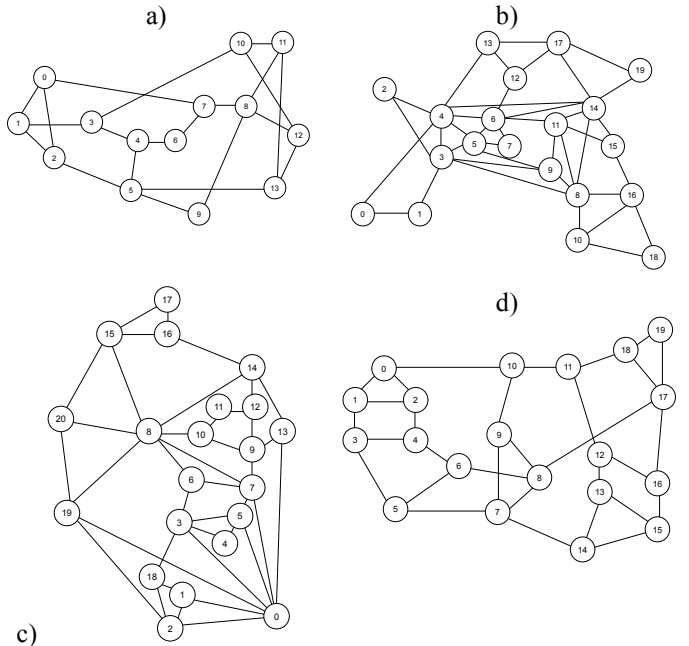


Figure 6: a) NSFNet, b) EON, c) UKNet and d) ARPANet topologies.

Table 2: Number of channels in the least and most loaded links (static and dynamic operation)

		Static	Dynamic (ρ)								
			0.1	0.2	0.3	0.4	0.5	0.6	0.7	0.8	0.9
NSFNet	Link,min	6	6	6	6	6	6	6	6	6	6
	Link,max	13	9	10	12	13	13	13	13	13	13
EON	Link,min	2	2	2	2	2	2	2	2	2	2
	Link,max	19	10	13	15	17	18	18	18	19	19
UKNet	Link,min	3	3	3	3	3	3	3	3	3	3
	Link,max	22	11	15	17	18	20	21	21	21	22
ARPANet	Link,min	5	4	5	5	5	5	5	5	5	5
	Link,max	34	14	18	23	27	30	33	33	33	34

In light of the results, the largest difference in the number of wavelengths in the static and dynamic cases is found at the maximum loaded link of the ARPANet topology: in the static case this link requires 34 wavelengths while the dynamic case

($\rho=0.1$) only requires a little less than half, namely 14. A change in 20 wavelengths could lead to a small Watt difference in the EDFA's power consumption. This difference can be easily taken into account using Eq. (7); however, its magnitude is not as high as to cause significant changes in the final results. Thus, we assume that $\Delta_{\text{links}} = 0$.

Figure 7 shows the total power consumption of the different node architectures for the EON topology configured as static (Equation (9) and (11)) and dynamic (Equation (13)) network as a function of the traffic load (traffic load as in Eq. (1)). The power consumption has been normalized to the value of P_L . Thus, the vertical axis is dimensionless. The values of ε and β are set to 0.1 and 1, respectively. This value of β means that SR and LR devices have the same power consumption. Increasing the parameter β would in practice mean a capacity upgrade of the network. The value used for ε represents that a device in the OFF-state only consumes 10% of the power when it is in the ON-state. Fractions in that order of magnitude have been reported in research for high-rate energy-efficient Ethernet considering a short-range optical transport layer [34]. It is assumed that a similar value of ε can be applied to long-range optical components. The value of ε may vary depending on the networking scenario and implementation of the short-range or long-range transmission circuits. Intuitively, any power saving mode should lead to a low value of ε . We may therefore expect with reasonable probability that ε will indeed be low for both short-range and long-range transmission circuits.

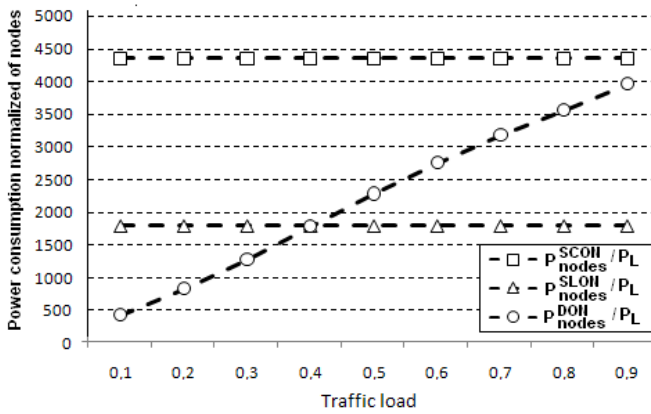


Figure 7. Power consumption normalized of nodes of the EON (dashed line) topology versus traffic load for SCON (square), SLON (triangle) and DON (circle) architectures, $\varepsilon=0.1$ and $\beta=1$.

Figure 7 shows that the power consumption of SCON and SLON architectures do not change with the traffic load. All the components are kept in the active state irrespective of their level of utilization. Instead, the power consumption of the DON architecture changes with the traffic load due to the load-dependent channel activation. It can also be seen that the DON architecture results in significant power savings with respect to the SCON architecture for all traffic loads. Compared to the SLON architecture, the DON architecture only achieves large power savings for loads well below 0.4. For traffic loads higher than 0.4, the number of wavelengths (transponders related to input/output stage) and transmitters/receivers of the dynamic case reaches that of the

static case, which makes the benefit of dynamic operation fade.

Results for the remaining topologies exhibit the same behaviour shown by EON in Figure 7 ($\varepsilon=0.1$ and $\beta=1$): dynamic operation becomes beneficial with respect to the static case for traffic loads under [0.36; 0.42]. The difference among the different topologies lies in the different number of nodes: topologies with a higher node-count consume more power due to the higher wavelength (transponders) and transmitter-receiver requirements, but the relative trends of the curves are the same.

The impact of the number of nodes is confirmed when taking the SCON consumption as reference and using it to normalize the SLON and DON consumption. In other words, equations (11) and (13) are divided by (9). As a result, the relative power consumption of an SLON compared to an SCON is as follows:

$$\frac{P_{\text{nodes}}^{\text{SLON}}}{P_{\text{nodes}}^{\text{SCON}}} = \frac{\beta \cdot W_{\text{net}}^{\text{SLON}}}{N(N-1) + W_{\text{net}}^{\text{SCON}}(\beta+1)} \quad (20)$$

This indicates that the advantage of SLON over SCON decreases rapidly for large networks and, most importantly, large values of β . Figure 7 clearly indicates that the relative advantage of DON over SCON is linearly dependent on the load, which is suggested by equation (13). As shown in Table 1, the number of transmitters and receivers as well as the number of wavelengths (transponders) is a load-dependent fraction of the number needed in SCON. The four networks studied have similar ratios such that the relative power savings of a DON over an SCON are comparable; however, a simple expression should be found for these load-dependent fractions and other networks should be evaluated.

Regarding the two static node architectures, it is clear that SLON consumes less energy than SCON; however, the achieved savings are not high enough so as to become an attractive alternative to the dynamic approach. When comparing previous results published in [35] with the ones presented in this work, the energy-efficiency of the dynamic scenario is higher here. Only $\beta=10$ was analyzed in [35]. The differences stem from:

- The dynamic case studied in [35] assumed $(N-1)$ transmitters and $(N-1)$ receivers per node. In this work however, the number of transmitters and receivers per node was dimensioned as a function of the traffic load and the maximum value of blocking per connection. In this way, a decrease in the power consumption of nodes of up to 5% (with respect to the dynamic case with $(N-1)$ transmitters/receivers) was achieved assuming $\beta=10$ for both cases.
- The static case in [35] assumed a static node architecture without regeneration capabilities. This assumption not only affected the power consumption of the node but also the technical feasibility of such a solution, especially in large-scale transport networks. In this paper, the static node architectures include regeneration capabilities. Therefore, the power consumption of nodes of the static architectures

studied in this paper (SCON and SLON) is up to 140% and 115% higher than that studied in [35] assuming $\beta=10$ for all cases, respectively (nodes in [35] have LR transmitters-receivers without transponders at input/output stages).

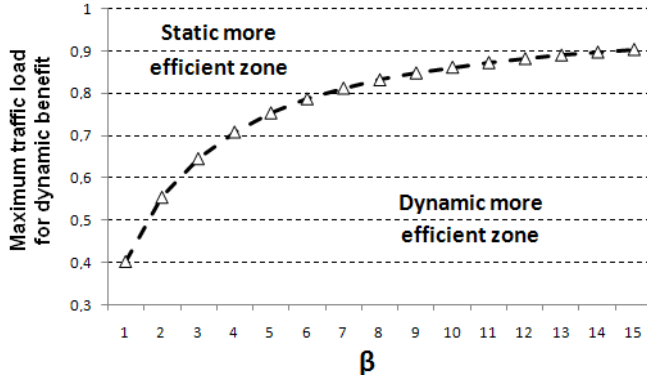


Figure 8: The β -dependence of the energy-efficiency in dynamic networks (SLON versus DON) for EON topology.

To study the impact that the value of β has on the benefit of dynamic operation in terms of power consumption, Figure 8 shows the value of traffic load at which the curve of the power consumption of the dynamic network (DON) becomes equal to that of the static network (SLON), as a function of the value of β for the EON topology. Thus, the area under the curve corresponds to the operation regime where dynamic operation is beneficial with respect to the static approach. It can be seen that as β increases because of capacity upgrades, the advantage of having load-dependent dynamic wavelength handling becomes more significant in terms of power consumption (increasing the traffic load at which dynamic operation saves more power than static operation from 0.4 for $\beta=1$ to 0.9 for $\beta=10$). In other words, the savings obtained by dynamic operation at low traffic loads increases with β . Exactly the same behaviour is observed for remaining topologies. This result is particularly interesting since most backbone networks are lightly utilized [36], as shown by recent OC-192 backbone traces available through CAIDA which show a load between 10% and 15% [37] and an IP link utilization of about 25% reported in [38]. Additionally, such low values of utilization are not envisaged to change, in spite of the constantly increasing Internet traffic, as comprehensively discussed in [39].

Finally, the impact of the power consumption of the interface and input/output stages of the node architectures on the migration from static to dynamic networks is evaluated by quantifying the values of $\Delta_{interface}$ and $\Delta_{input,output}$ for SLON and DON architectures. Only the SLON and DON architectures are considered here as Figure 7 clearly indicates that the SLON is more energy-efficient than the SCON. Figure 9 shows the value of $\Delta_{interface}$ (square) and $\Delta_{input,output}$ (triangle) normalized to the value of P_L for the EON topology, for $\varepsilon=0.1$, and for values of β equal to 1 (Figure 9.a) and 10 (Figure 9.b). Positive values indicate the convenience of a dynamic architecture.

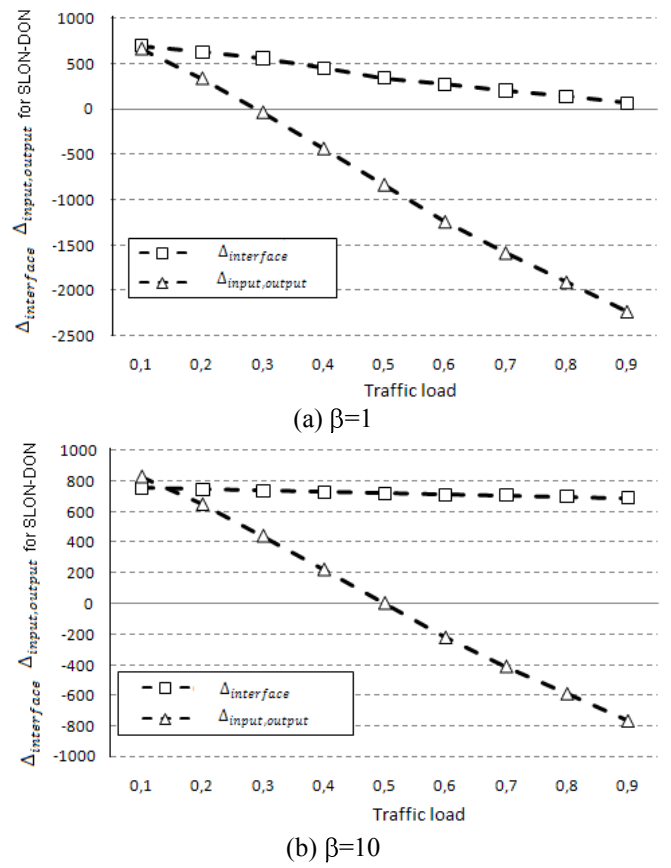


Figure 9: Power savings when replacing SLON with DON nodes in the EON network. $\Delta_{interface}$ (square) and $\Delta_{input,output}$ (triangle) are considered separately.

From Figure 9 it can be seen that the input and output stages determine the benefit of an eventual migration from static to dynamic architecture, as the interface stage always achieves a positive value for $\Delta_{interface}$. As the DON interface stage only consists of SR devices, it always offers a power saving with respect to the SLON case (made of LR devices); however, the variance is not so great with respect to the offered traffic load, which can be intuitively understood when comparing the node designs in Figures 2 and 3. The same behavior is observed in remaining topologies.

In terms of the benefit of the migration, results of Figure 9(a)-(b) correspond to results shown in Figures 7 and 8. The dynamic node architectures offer power savings over static node architectures at low network loads and increasing values of β . Regarding the input/output stage power consumption, a significant change in the difference between the power consumption of static and dynamic architectures is observed as the traffic load increases. Similar to Figures 7 and 8, the dynamic nodes do not offer a power savings when a particular traffic load is exceeded. This is due to a higher component count in the DON than in the SLON. Increasing the value of β gives a similar advantage to DON architectures as previously observed; however, the break-even point is shifted to higher loads.

It may be concluded from Figure 9 that when dimensioning a dynamic WDM network, more importance should be given to a reduction in the number of wavelengths (transponders of input and output stage) than in the number of transmitters and receivers, in terms of energy-efficiency. The reader should note that the ϵ only takes into account the optical transport layer and not the full-scale host.

VI. CONCLUSION

In this work the power consumption of WDM networks operating in static or dynamic modes was evaluated. For this purpose, a general framework to model energy consumption of nodes and links was proposed and discussed. This framework enables the analysis of different scenarios where different node architectures, link capacities and network topologies can be considered. In the case of the static network, two node architectures were evaluated: a classical one (SCON) and a second one which requires a decreased number of transponders (SLON). In the dynamic case, an architecture (DON), which allows full reconfigurability was considered. Four network topologies were studied: NSFNet, EON, UKNet and ARPANet.

In the static case, it was shown how much less energy the SLON architecture consumes with respect to the SCON one due to the elimination of redundant transponders. In general, dynamic operation resulted in a significant reduction in power consumption with respect to the static case. If long and short reach transponders consume about the same power, dynamic operation is beneficial only at low values of traffic loads (<0.4). However, if short reach transponders consume much less power than long reach ones, dynamic operation becomes more energy efficient for traffic loads of up to 0.9.

In this analysis, the difference in power consumption between the sleep and active modes is assumed at 90%. It should be noted that smaller differences lead to less significant benefits of introducing dynamic network operation, and therefore the results may vary depending on the transport technology and system design.

Finally, it is also shown that the transponders of the input/output stage of the nodes determine the benefit –in terms of power consumption- of an eventual migration from static to dynamic architecture rather than the transponders of the interface between the WDM and higher layers.

These trends were observed for all topologies studied.

We can conclude that WDM dynamic operation has much potential in contributing to decreasing the energy consumption of telecommunication networks. We expect that these results will help network operators and network equipment designers decide whether to use static or dynamic optical nodes.

Further research would include the impact of optimal regenerator placement on power consumption of WDM networks, and measured characteristics of EDFA's power consumption.

REFERENCES

- [1] P. Yuan and A. Xu, "The influence of physical network topologies on wavelength requirements in optical networks", IEEE/OSA J. Lightw. Technol., vol. 28, no. 9, May 1, 2010.
- [2] IETF, "RFC 3471 - Generalized Multi-Protocol Label Switching (GMPLS) Signaling Functional Description," January 2003.
- [3] ITU, "Rec. G.8080/Y.1304: Architecture for the automatically switched optical network (ASON)," February 2005.
- [4] A. Zapata-Beghelli and P. Bayvel, "Dynamic Versus Static Wavelength-Routed Optical Networks", IEEE/OSA J. Lightw. Technol., vol. 26, no 20, pp. 3403–3415, Oct. 2008.
- [5] A. Beghelli, A. Leiva, R. Vallejos, M. Aravena, "Static vs. dynamic WDM optical networks under single-cable failure conditions", in Proc. of the 13th international conference on Optical Network Design and Modeling ONDM, pp. 111-116, Braunschweig, Germany, 2009.
- [6] A. Leiva, A. Beghelli, "Wavelength requirements of fault tolerant static and dynamic WDM networks", in Proc. of the 14th European Conference on Networks and Optical Communications and 4th Conference on Optical Cabling and Infrastructure NOC/OC&I, pp. 209-216. Valladolid, Spain, 2009.
- [7] Gupta, M. and Singh, S, "Greening of the internet", in Proc. of the Conference on Applications, Technologies, Architectures, and Protocols for Computer Communications SIGCOMM, pp. 19-26, Karlsruhe, Germany, 2003.
- [8] G. Shen, "Evolution of WDM Optical IP Networks: A Cost and Energy Perspective", OSA/IEEE J. Opt. Commun. Netw. vol.1 no 1, pp. 176-186, 2009.
- [9] S. Aleksic, "Analysis of Power Consumption in Future High-Capacity Network Nodes", OSA/IEEE J. Opt. Commun. Netw. vol. 1, no. 3, pp.245-258, 2009.
- [10] E. Bonetto, L. Chiaravaglio, D. Cuda, G. A. Gavilanes Castillo, F. Neri, "Optical technologies can improve the energy efficiency of networks", Eur. Conf. Exhib. Opt. Commun., Paper 5.5.1, 2009.
- [11] R. S. Tucker, R. Parthiban, J. Baliga, K. Hinton, R. W. A. Ayre, and W. V. Sorin "Evolution of WDM Optical IP Networks: A Cost and Energy Perspective". IEEE/OSA J. Lightw. Technol., vol. 27, no 3, pp. 243 – 252, 2009.
- [12] I. Cerutti, L. Valcarenghi, P. Castoldi, "Power Saving Architectures for Unidirectional WDM Rings", in Proc. of Optical Fiber Conference (OFC) 2009, post deadline paper, San Diego, California USA, 2009.
- [13] E. Bonetto, D. Cuda, G.A. Gavilanes Castillo, and F. Neri, "The role of arrayed waveguide gratings in energy-efficient optical switching architectures", in Proc. Optical Fiber Conference (OFC) 2010, paper OWY4, San Diego, CA, USA, Mar. 2010.
- [14] A. Silvestri, A. Valenti, S. Pompei, F. Matera, A. Cianfrani, and A. Coiro, "Energy saving in optical transport networks exploiting transmission properties and wavelength path optimization", Optical Switching and Networking, vol. 7, no 3, pp. 108-114, July 2010.
- [15] S. Baroni and P. Bayvel, "Wavelength requirements in arbitrarily connected wavelength-routed optical networks", IEEE/OSA J. Lightw. Technol., vol. 15, no 2, pp. 242–251, Feb. 1997.
- [16] M. Dürer and P. Bayvel, "Analysis of a dynamically wavelength-routed optical burst switched network architecture," IEEE/OSA J. Lightw. Technol., vol. 20, no. 4, pp. 574–585, Apr. 2002.
- [17] J. He and D. Simeonidou, "A flow-routing approach for optical IP networks", in Proc. of Optical Fiber Conference (OFC) 2001, vol. 1, pp. MN 2-2 - MN2-3, 2001.
- [18] A. Zapata, I. de Miguel, M. Dürer, J. Spencer, P. Bayvel, D. Breuer, N. Hanik, A. Gladish, "Next Generation 100-Gigabit Metro Ethernet (100GbME) using multiwavelength optical rings". IEEE/OSA J. Lightw. Technol., vol. 22, no 11, pp. 2420-2434, Nov. 2004.
- [19] J. H. Siregar, H. Takagi, Y. Zhang, "Fast routing and wavelength assignment heuristics of large-scale WDM optical networks", IEICE Trans. Commun., vol. E86-B, no 12, pp. 3530–3537, Dec. 2003.
- [20] Y. Ye, H. Zhang, T. Qin, W. Dai, F. Feng, X. Huo, Y. Guo, "Statistics study of routing and wavelength assignment algorithms in WDM all optical network", Optics Commun., vol. 185, no 4, pp. 315–320, Nov. 2000.
- [21] Y. Huang, D. Datta, X. Qiu, J. Zhang, HK. Park, YC. Kim, JP. Heritage, B. Mukherjee, "Studies on a Class of AWG-Based Node Architectures for Optical Burst-Switched Networks", in Proc. International Conference on Computational Science, pp. 1224-1232, 2004.

- [22] M.C. Wu, O. Solgaard, and J.E. Ford, "Optical MEMS for lightwave communication", in IEEE/OSA J. Lightw. Technol., vol. 24, no. 12, pp. 4433-4454, Dec. 2006 (invited).
- [23] ITU-T, "Physical transfer functions of optical network elements", G.680 Recommendation, July, 2007. Available online: <http://www.itu.int/rec/T-REC-G.680/en>.
- [24] Y. Sun, A.K. Srivastava, J. Zhou, and J.W. Sulhoff, "Optical fiber amplifiers for WDM optical networks", in Bell Labs Technical Journal, vol. 4, no. 1, pp. 187-206, January-March 1999.
- [25] P.C. Becker, N.A. Olson, and J.R. Simpson, "Erbium-doped fiber amplifiers: fundamentals and theory", Academic Press, 1999.
- [26] Home page of Furukawa Electric, Pump Lasers section. Available online: <http://www.furukawa.co.jp/fitel/eng/active/pumping.html>
- [27] Home page of JDS Uniphase, Optical Pumping section. Available online: <http://www.jdsu.com/products/commercial-lasers/applications/optical-pumping.html>
- [28] S.Y. Park, H.K. Kim, G.Y. Lyu, S.M. Kang, and S.-Y. Shin, "Dynamic gain and output power control in a gain-flattened Erbium-doped fiber amplifier", in IEEE Photon. Technol. Lett., vol. 10, no. 6, pp. 787-789, June 1998.
- [29] Finisar FTLX1371D3BCL and FTLX1471D3BCL 10G SFP+ transceivers. Available: <http://www.finisar.com/products/optical-modules/sfp-plus>
- [30] D. Banerjee, B. Mukherjee, "A Practical Approach for Routing and Wavelength Assignment in Large Wavelength- Routed Optical Networks", IEEE J. Sel. Areas in Commun., vol. 14, no. 5, pp.903-908, Jun. 1996.
- [31] O. Gerstel, G. Sasaki, S. Kutten, R. Ramaswami, "Worst-Case Analysis of Dynamic Wavelength Allocation in Optical Networks", IEEE/ACM Trans. Netw., vol. 7, no. 6, pp. 833-845, Dec. 1999.
- [32] N. Seitz, "ITU-T QoS standards for IP-based networks", IEEE Commun. Mag., vol. 41, no 6, pp.82-89, Jun. 2003.
- [33] ITU Recommendation E.721, "Network grade of service parameters and target values for circuit-switched service in the evolving ISDN", May 1999.
- [34] P. Reviriego, B. Huiszoon, V. López, R.B. Coenen, J.A. Hernández, and J.A. Maestro, "Improving energy-efficiency in IEEE 802.3ba high-rate Ethernet optical links" scheduled for publication in Special Issue on Green Photonics of the IEEE Journal of Selected Topics in Quantum Electronics, pp. 1-9 , DOI: 10.1109/JSTQE.2010.2050136.
- [35] A. Leiva, J. M. Finochietto, V. López, B. Huiszoon, A. Beghelli, "Comparison of Static and Dynamic WDM Networks in Terms of Energy Consumption", in Proc. Optical Fiber Conference (OFC) 2010, paper JThA44, San Diego, CA, USA, March. 2010.
- [36] C. Fraleigh, S. Moon, B. Lyles, C. Cotton, M. Khan, D. Moll, R. Rockell, T. Seely and S.C. Diot, "Packet-level traffic measurements from the Sprint IP backbone," IEEE Network, vol.17, no.6, pp. 6- 16, December 2003.
- [37] C. Walsworth, E. Aben, K.C. Claffy, and D. Andersen, The CAIDA anonymized 2009 Internet traces, 15th January 2009. Available (online, May 2010): http://www.caida.org/data/passive/passive_2009_dataset.xml.
- [38] A. A. M. Saleh, J. Simmons, "Technology and Architecture to Enable the Explosive Growth of the Internet", IEEE Communications Magazine, vol. 49, no. 1, pp. 126-132, January 2011.
- [39] A.M. Odlyzko, "Data networks are lightly utilized, and will stay that way" in Review of Network Economics, vol. 2, no. 3, pp. 210-237, Sept. 2003.